Dynamics of Low-Spin Baryon States*

E. Golowich

Carnegie Institute of Technology, Pittsburgh, Pennsylvania

(Received 15 August 1966)

We study baryon states of spin $\leq \frac{3}{2}$ using a dynamics based on an approximation to the Bethe-Salpeter equation which includes baryon and meson-exchange forces. Considering only S- and P-wave vertices, we perform a multichannel calculation using an $SU(6)$ description. A solution to a $56^+:70^-$ bootstrap model (superscript denotes parity) is found which qualitatively reproduces the experimental coupling constants and has a mass difference, $M(70) - M(56) = 260$ MeV. Analysis of symmetry-breaking effects in this model gives qualitative agreement with experiment. A solution to a $56^+:70^-:20^+$ bootstrap is found with 56^+, 70^-, 20^+ approximately degenerate, thus supplying theoretical evidence for the existence of 20^+ in nature. The multiplet 20^- is found to exist only with a $56^+:70^-:20^+:20^-$ model. A separate study of long-range forces in pseudoscalar meson-baryon scattering predicts an effect in the isospin-zero $P_{1/2}$ wave of the KN system and possibly the occurrence of a family of $P_{1/2}$ resonances belonging to the $SU(3)$ mutliplet, $\overline{10}$, but not containing the Roper effect.

1. INTRODUCTION

RECENT phase-shift analyses of the πN system[1] have exhibited the existence of resonances in S, P, D, F, and G waves, and there is evidence from total cross-section and backward-scattering measurements[2] for resonances of even higher spin. A most interesting feature of this abundant spectrum is the appearance of families of particles with the same parity, different strangeness, and roughly equal mass. In addition, there is a striking amount of inelasticity present in the resonance region which, for the most part, has not been satisfactorily explained by various theoretical models. The work described here is an attempt to at least partially account for the above experimental effects by studying S- and P-wave dynamics of states with baryon number one and angular momentum $\leq \frac{3}{2}$. There are two reasons for partitioning the particle spectrum in this manner: (i) the states with small angular momentum have relatively low mass, so, as a practical matter, one expects these states to have the simplest structure because of the small number of open channels; (ii) there is hope that having understood the nature of the "ground states," we might gain insight into the dynamics of the "excited states" in a relatively straightforward manner.[3,4]

Since the particle spectrum is closed under experiment in the sense that no radically different type of entity (with, say, nonintegral charge or baryon number) has yet been observed, a natural explanation of the baryonic states appears to be given by the bootstrap dynamics. In this paper, we carry out a series of bootstrap calculations based on vertex and normalization

equations as developed by Cutkosky and Leon.[5,6] Since we wish to account for some of the inelasticity observed in scattering experiments, we adopt a multichannel approach, using $SU(6)$ to facilitate description of particle multiplets and correlation of interaction vertices. Unlike many current papers employing higher symmetries, we require that the $SU(6)$ satisfy the consistency conditions imposed by the dynamics, i.e., the symmetry appears as a consequence of the forces.

To summarize the contents, Sec. 2 contains a detailed discussion of the model, Secs. 3 and 4 involve specific applications, Sec. 5 is devoted to a discussion of a low-angular-momentum effect recently seen in the KN system, and Sec. 6 contains conclusions and a discussion of the results.

2. DISCUSSION OF THE MODEL

This section is divided into two parts, the first of which surveys our dynamical model, while the second discusses the role $SU(6)$ plays in our calculations.

We base our dynamics on a bound-state description of particles given by the Bethe-Salpeter equation.[5,6] As seen in Fig. 1, vertex and normalization conditions are described by single-particle exchange graphs. Taking external particles on the mass shell and approximating all vertices by coupling constants, we generate a set of bootstrap equations relating coupling constants and mass differences. In short, the vertex equations represent an average over momentum of various Born terms, with the important constraint that the equations are symmetric with respect to interchange of the external baryons, a feature not generally seen in the familiar N/D approach.[6] The vertex and normalization equations have the form

$$g_{ab} = \sum_{e,f} g_{af} g_{eb} g_{ef} D^{(i)}{}_{ab}{}^{ef}, \tag{1a}$$

$$N_a = \sum_{b,e,f} g_{af} g_{eb} g_{ef} g_{ab} W^{(i)}{}_{bf}{}^{ae} \tag{1b}$$

* Supported in part by the U. S. Atomic Energy Commission.

[1] B. H. Bransden *et al.*, Phys. Rev. **139**, B1566 (1965); Phys. Letters **19**, 420 (1965); P. Bareyre *et al.*, *ibid.* **18**, 342 (1965); A. Donnachie *et al.*, *ibid.* **19**, 149 (1965).

[2] A. Citron *et al.*, Phys. Rev. **144**, 1101 (1966); S. W. Kormanyos *et al.*, Phys. Rev. Letters **26**, 709 (1966).

[3] P. A. Carruthers, Phys. Rev. **133**, B497 (1964); Phys. Rev. Letters **12**, 259 (1964).

[4] E. Golowich, Phys. Rev. **139**, B1297 (1965).

[5] R. E. Cutkosky and M. Leon, Phys. Rev. **135**, B1445 (1964); **138**, B667 (1965).

[6] K. Y. Lin and R. E. Cutkosky, Phys. Rev. **140**, B205 (1965).

for baryon exchange processes and

$$g_{ab}=\sum_c g_{ac}g_{cb}g_\mu D^{(i)}{}_{ab}{}^c, \quad (2a)$$

$$N_a=\sum_{b,c} g_{ab}g_{bc}g_{ca}g_\mu W^{(i)}{}_{bc}{}^a, \quad (2b)$$

for meson exchange, where the superscript i implies that two distinct types of dynamical factors, $D^{(i)}$, can occur because of the existence of S- and P-wave vertices. Explicit forms of the $D^{(i)}$ factors are given here:

baryon exchange—

$$D^{(1)}{}_{ab}{}^{ef}=\frac{1}{12\pi^2}\int_\mu^\Lambda \frac{k^3 d\omega}{(\omega+M_f-M_a)(\omega+M_e-M_b)} \times C_{ab}{}^{ef}, \quad (3a)$$

$$D^{(2)}{}_{ab}{}^{ef}=\frac{1}{4\pi^2}\int_\mu^\Lambda \frac{k d\omega}{(\omega+M_f-M_a)(\omega+M_e-M_b)}C_{ab}{}^{ef}; \quad (3b)$$

meson exchange—

$$D^{(1)}{}_{ab}{}^c=\frac{1}{12\pi^2}\int_\mu^\Lambda \frac{k^3 d\omega}{(\omega+M_c-M_a)(\omega+M_c-M_b)}C_{ab}{}^c, \quad (4a)$$

$$D^{(2)}{}_{ab}{}^c=\frac{1}{4\pi^2}\int_\mu^\Lambda \frac{k d\omega}{(\omega+M_c-M_a)(\omega+M_c-M_b)}C_{ab}{}^c, \quad (4b)$$

where M_i are baryon masses, μ is the average meson mass, ω is the meson energy, the factors $C_{ab}{}^{ef}$, $C_{ab}{}^c$ are proportional to crossing coefficients, and the same cutoff, Λ, is used for all integrals. A class of crossing coefficients not available in the literature but relevant to the above equations is calculated in Appendix A and an explicit derivation of one of the $D^{(i)}$ is given in Appendix B. The normalization factors $W^{(i)}$ are too numerous to list explicitly, but are evaluated in a man ier similar to those discussed in Ref. 6. The bootstrap equations are simplified by expanding both vertex and normalization dynamical factors to first order in the baryonic mass differences. Explicit spin dependence of propagators is suppressed since we employ static-like nonrelativistic kinematics, and also use an $SU(6)$ description for the particles.

We now discuss the assignment of physical particles to $SU(6)$ multiplets, considering first a vertex consisting of one mesonic and two baryonic particles. An $SU(6)$ multiplet may be written as a direct sum of submultiplets labelled by (U,J), where U, J denote the dimensionality of $SU(3)$ and $SU(2)$ multiplets, respectively, the latter corresponding to an angular momentum. For fermions, we take this angular momentum as the spin, e.g., the baryon octet is assigned to $(8,2)$. The assignment of negative-parity mesons is based on j-j coupling[7] and thus depends on the relative intrinsic parity of the two baryons. Consider a vertex coupling of a pseudoscalar meson to two spin-$\frac{1}{2}$ baryons of opposite relative parity. By conservation of parity, the allowed orbital angular momenta are $l=0, 2, 4, \cdots$. Conservation of

angular momentum implies $l=0$ or 1, and hence the meson appears in an $l=0$ state. Since, for j-j coupling, $\mathbf{j}(\text{meson})=\mathbf{l}+\mathbf{s}(\text{meson})$, then $\mathbf{j}=\mathbf{s}$ and the following assignments obtain: vector meson octet $(8,3)$; pseudoscalar octet $(8,1)$; vector meson singlet $(1,3)$, all of which forms a **35**. When the baryons have the same relative parity, conservation of angular momentum and parity plus a requirement that the mesons be assigned to **35** implies $l=1$. However, submultiplet assignments are not unique here, since we can form $j=1$ states from both $\nabla\varphi$ and $\nabla\times\mathbf{V}$, where φ, $\mathbf{V}$ are pseudoscalar and vector-meson states, respectively.[8] In general, we must write $(8,3)=\alpha_8\nabla\varphi_8+\beta_8\nabla\times\mathbf{V}_8$ and $(1,3)=\alpha_1\nabla\varphi_1+\beta_1\nabla\times\mathbf{V}_1$ in assigning mesons to **35** for a P-wave vertex. This ambiguity may be eliminated if we adopt a particular dynamical model. In the calculations to follow, we take $\alpha_8=\alpha_1=1/\sqrt{3}, \beta_8=\beta_1=\sqrt{2}/\sqrt{3}$, a choice which comes from a Fermi-Yang model of the mesons and also from W spin. The only way to fill $(8,1)$ for a P-wave vertex is with $\nabla\cdot\mathbf{V}$, which represents a coupling of $l=1$ and $s=1$ to form $j=0$.

Since the trimeson vertex has rather different kinematics from the vertices discussed above, our discussion does not proceed along the same line of reasoning. Instead, we define this interaction in a manner described by Capps, based on W spin. The vertex thus defined is Lorentz invariant, obeys permutation symmetry, and is self-consistent within a bootstrap model.[9] We normalize these couplings with the $\rho\pi\pi$ decay width.

We conclude this section with some general remarks about the model. The physical origin of the $SU(6)$ operators that we use to describe baryonic vertices lies in an extension of the Chew-Low model. It is therefore natural that we assign mesons to **35** according to their total angular momentum in the baryon rest frame. Since we are forced to use nonrelativistic kinematics in view of the above picture, our numerical results have at best semiquantitative significance. However, this defect is more than offset by our need for $SU(6)$ in carrying out a multichannel analysis, which would otherwise be too cumbersome. In addition, the baryonic spectrum has proved such a difficult problem that, in general, even a qualitative understanding of it is still lacking, and thus previous success of $SU(3)$ and $SU(6)$ in classifying particle multiplets gives us further incentive to use $SU(6)$ here.

3. 56⁺:70⁻ BOOTSTRAP MODEL

Our first application is to a **56⁺:70⁻** reciprocal bootstrap [the superscripts denote the parity of the $SU(6)$ multiplet]. The chief experimental motivation for studying the existence of **70⁻** comes from recent analyses of πN phase shifts,[1] which indicate the existence of S_{11}, S_{31}, and D_{13} resonances (we use the notation $L_{2T,2J}$,

[7] R. H. Capps, Phys. Rev. Letters **14**, 31 (1965); J. G. Belinfante and R. E. Cutkosky, ibid. **14**, 33 (1965).

[8] J. G. Belinfante and G. H. Renninger, Phys. Rev. **148**, 1573 (1966).

[9] R. H. Capps, Phys. Rev. **144**, 1182 (1966); **148**, 1332 (1966); Bull. Am. Phys. Soc. **11**, 369 (1966).

where T, J are the isospin and spin quantum numbers, respectively). Along with the $S_{01}Y_0^*(1405)$, this set of observed particles supplies at least one candidate for each submultiplet of 70^-, whose content is $70^- = (8,4)^- \oplus (8,2)^- \oplus (10,2)^- \oplus (1,2)^-$. The identification of 56^+, whose content is $(8,2)^+ \oplus (10,4)^+$ with physical particle states is, of course, complete. The theoretical motivation for this model comes from a study of the relevant $SU(6)$ crossing matrices,[10,11] where one finds rather large attractions and no repulsions occurring for both baryon- and meson-exchange graphs.

Before we introduce the bootstrap equations, a short review of previous models for states in 70^- is given, since to a certain extent, the forces we consider here have not yet been studied. The usual explanation for the $(8,4)^-$ states is the Cook-Lee[12] model of strongly coupled D-wave baryon–pseudoscalar-meson and S-wave baryon–vector-meson composites held together by meson exchange. One also sees attempts to use the nucleon-exchange pole leading to 3-3 isobar production. Both of these, which acknowledge the inelasticity of the $(8,4)^-$ resonances with respect to the incoming meson-baryon scattering state, involve D waves and so are excluded from our model. The best known model for the $Y_0^*(1405)$, classified in this paper as $(1,2)^-$, is that of Dalitz and Tuan,[13] who use an $N\bar{K}$ S-wave bound-state description. This possibility is included in our calculation, although only as a small part, since the $SU(6)$ Clebsch-Gordan coefficient[14] for the $Y_0^*\bar{K}N$ vertex is $(32)^{-1/2}$. Capps has repeatedly stressed the importance of meson-exchange forces in generating the 70^- multiplet as an S-wave $56^+ \otimes 35^-$ composite.[15] While agreeing with this viewpoint and including it in our model, we believe an understanding of S-wave resonances with this mechanism alone is difficult to justify. By including the $70^- \otimes 35^-$ P-wave composite, we have a natural resonance-generating mechanism with a long-range attractive force and a centrifugal barrier.

We now turn to the calculation. There are three vertices, two P wave, $g(56^+; 56^+; 35^-)$, $g(70^-; 70^-; 35^-)$ and one S wave, $g(70^-; 56^+; 35^-)$. The $70^-:70^-:35^-$ vertex is not unique, since the product $70^- \otimes 35^-$ contains 70^- twice. However, in a bootstrap model where the 70^- self-exchange force accounts for an appreciable part of the $70^-:70^-:35^-$ vertex, it can be shown[11] that the antisymmetric coupling of 70^- to $70^- \otimes 35^-$, which is proportional to the $SU(6)$ generators, dominates, and is thus used in this paper. Defining the dimensionless coupling constants $g_0 = (D^{(1)}{}_2)^{1/2}g(56^+; 56^+; 35^-)$, $g_0 = (D^{(2)}{}_2)^{1/2}g(70^-; 56^+; 35^-)$, $g_2 = (D^{(1)}{}_2)^{1/2}g(70^-; 70^-; 35^-)$, and mass difference $x = (M[70] - M[56])D^{(2)}{}_3/D^{(2)}{}_2$, where

$$D^{(1)}{}_n = \frac{1}{12\pi^2}\int_\mu^\Lambda \frac{k^3 d\omega}{\omega^n},$$ (5a)

$$D^{(2)}{}_n = \frac{1}{4\pi^2}\int_\mu^\Lambda \frac{k d\omega}{\omega^n},$$ (5b)

we have the following bootstrap equations:

$$g_0 = \frac{11}{15}g_0^3 + \frac{9}{4}\left(\frac{5}{33}\right)^{1/2}g_1^2 g_2(1-2x) + \frac{1}{2}\left(\frac{8}{15}\right)^{1/2}g_0^2 g_\mu + \frac{3}{8}\left(\frac{10}{3}\right)^{1/2}g_1^2 g_\mu(1-2x),$$

$$g_1 = \left[\frac{g_1^2}{4} + \frac{9}{5}\left(\frac{5}{33}\right)^{1/2}g_0 g_2 + \frac{3}{4}\left(\frac{8}{15}\right)^{1/2}g_0 g_\mu\left(1+\frac{x}{\gamma}\right) + \frac{1}{2}\left(\frac{2}{11}\right)^{1/2}g_2 g_\mu\left(1-\frac{x}{\gamma}\right)\right]g_1,$$

$$g_2 = \frac{7}{11}g_2^3 + \frac{9}{5}\left(\frac{5}{33}\right)^{1/2}g_1^2 g_0(1+2x) + \left(\frac{2}{11}\right)^{1/2}g_2^2 g_\mu + \frac{1}{2}\left(\frac{2}{11}\right)^{1/2}g_1^2 g_\mu(1+2x),$$

$$\frac{D^{(1)}{}_2{}^2}{D^{(1)}{}_3 K_0} = \frac{11}{15}g_0^4 + \frac{5\gamma}{16}(1-2x-\eta x)g_1^4 + \frac{9}{4}\left(\frac{5}{33}\right)^{1/2}\gamma(1-3\eta x)g_0 g_1^2 g_2 + \frac{9}{4}\left(\frac{5}{33}\right)^{1/2}(1-2x)g_0 g_1^2 g_2$$

$$+ \frac{5}{8}\left(\frac{2}{11}\right)^{1/2}\left(1-2x-\frac{3x}{\gamma}\right)g_1^2 g_2 g_\mu + \frac{3}{8}\left(\frac{10}{3}\right)^{1/2}\gamma(1-3\eta x)g_0 g_1^2 g_\mu + \frac{3}{8}\left(\frac{10}{3}\right)^{1/2}(1-2x)g_1^2 g_0 g_\mu + \frac{1}{2}\left(\frac{8}{15}\right)^{1/2}g_0^3 g_\mu$$

$$= \frac{7}{11}g_2^4 + \frac{\gamma}{4}(1+\eta x+2x)g_1^4 + \frac{9}{5}\left(\frac{5}{33}\right)^{1/2}\gamma g_0 g_1^2 g_2(1+3\eta x) + \frac{9}{5}\left(\frac{5}{33}\right)^{1/2}(1+2x)g_0 g_1^2 g_2$$

$$+ \frac{3}{4}\left(\frac{8}{15}\right)^{1/2}g_1^2 g_0 g_\mu\left(1+2x+\frac{3x}{\gamma}\right) + \frac{1}{2}\left(\frac{2}{11}\right)^{1/2}\gamma g_2 g_1^2 g_\mu(1+3\eta x) + \frac{1}{2}\left(\frac{2}{11}\right)^{1/2}g_2 g_1^2 g_\mu(1+2x) + \left(\frac{2}{11}\right)^{1/2}g_\mu g_2^3,$$ (6)

[10] V. Singh and B. M. Udgaonkar, Phys. Rev. 139, B1585 (1965).
[11] E. Golowich (unpublished).
[12] T. C. Wong, Clarendon Laboratory report, 1966 (unpublished), and references cited therein.
[13] R. H. Dalitz and S. F. Tuan, Ann. Phys. (N. Y.) 10, 307 (1960).
[14] C. L. Cook and G. Murtaza, Nuovo Cimento 39, 531 (1965).
[15] R. H. Capps, Phys. Rev. 139, B421 (1965); Phys. Rev. Letters 14, 842 (1965).

where g_μ represents a dimensionless trimeson coupling constant, $\Lambda = 1.05$ BeV,

$$\gamma = [D^{(1)}{}_2 D^{(2)}{}_3]/[D^{(1)}{}_3 D^{(2)}{}_2],$$

and

$$\eta = [D^{(2)}{}_2 D^{(2)}{}_4]/[D^{(2)}{}_3]^2. \tag{7}$$

A solution of this set of nonlinear equations was found with $g_0 = 0.87$, $g_1 = 0.525$, $g_2 = 0.55$, $x = 0.26$ (no other solution was found). The most important contributions to each vertex are shown in Fig. 2. The $56^+ : 56^+ : 35^-$ vertex is dominated by the 56^+ exchange graph and the meson exchange force in elastic $56^+ \otimes 35^-$ scattering. This is in accord with previous models of this vertex employing lower symmetries, and also points out the importance of meson-exchange forces in describing the dynamics of the baryon states. Another interesting feature of the solution is the near equality of the S wave $70^- : 56^+ : 35^-$ and P wave $70^- : 70^- : 35^-$ vertices. Since we fix the cutoff Λ of the $D_n{}^{(i)}$ [see 5(a), (b)] by normalizing the $56^+ : 56^+ : 35^-$ vertex to give the experimental value of the $NN\pi$ coupling constant, we can compare the theoretical $70^- : 56^+ : 35^-$ coupling constant with the experimental value as given by, for instance, the $Y_0^*(1405) \to \Sigma\pi$ decay width. Using a simple S wave Breit-Wigner fit to the scattering amplitude, we have

$$g_{Y:\Sigma:\pi}{}^2/4\pi = \tfrac{1}{2}\Gamma/k, \tag{8}$$

where Γ is the decay width and k the final momentum in the Y_0 rest frame. We find $g_1(\text{expt.}) = 0.38$ while $g_1(\text{theory}) = 0.52$, which is within the order-of-magnitude agreement we ask of our results. A further comparison of $SU(6)$ predictions for the decay of particles in 70^- and the corresponding experimental widths is given in Appendix C. Possible experimental determination of the coupling $g(70^-; 70^-; 35^-)$ is meager at this time, but recent indications[16] of the importance of the $Y_1^*(1660) \to Y_0^*(1405)\pi$ decay mode is consistent with our result.

(a)

(b)
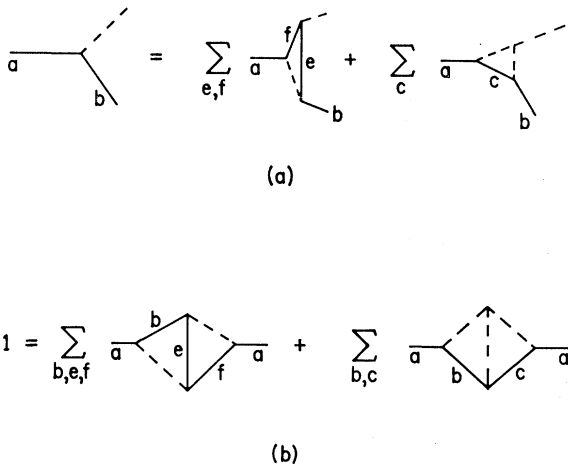
FIG. 1. Vertex (a) and normalization (b) equations.

[16] P. Eberhard *et al.*, Phys. Rev. Letters **14**, 466 (1965); and R. R. Rau, Phys. Rev. **143**, 1034 (1966).
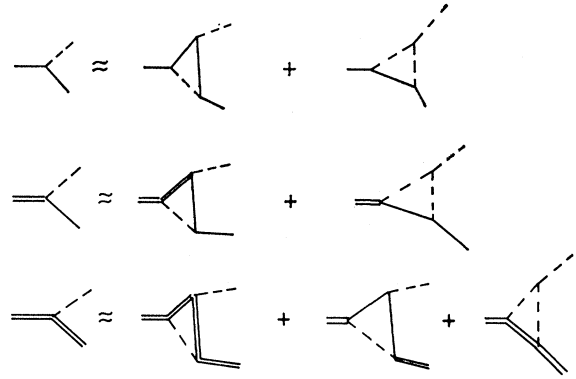
FIG. 2. Graphs in the $56^+ : 70^-$ vertex equations with large coefficients. Single, double, and dashed lines represent 56^+, 70^-, and 46^-, respectively.

The mass difference between 56^+ and 70^- corresponding to $x = 0.26$ is 260 MeV and is of the correct sign.

Since our dynamics relies heavily upon the notion of self-consistency, it is essential that the solution to the bootstrap equations not imply any larger set of particles than was originally put into the model. We study this point by determining the eigenvalues of the "potential matrix" as described in Ref. 6. The basic idea is that the bootstrap equations can be considered a mapping of coupling constants

$$(g_a)_b = \sum_f V_{bf}(a)(g_a)_f, \tag{9a}$$

where

$$V_{bf}(a) = \sum_e g_{cb} g_{ef} D_{ab}{}^{ef} + \sum_\mu g_{fb} g_\mu D_{ab}{}^f. \tag{9b}$$

In a given channel, self-consistency occurs if the transformation V has an eigenvalue of unit magnitude and all others smaller. The $56^+ : 70^-$ solution discussed above has a potential matrix with the following eigenvalues in the 56^+, 70^- direct channels: $\lambda_{56} = 1.0$, -0.02 and $\lambda_{70} = 1.0$, -0.02. Hence, this solution definitely satisfies the self-consistency criterion.

A consequence of the use of $SU(6)$ symmetry is the occurrence of degenerate multiplets of particles. The extent to which we can reproduce the qualitative features of the actual mass spectrum is an important point which we now discuss.[17] Probably the simplest and crudest approach is the "effective-threshold" method where one writes a Clebsch-Gordan expansion for some state, uses real masses for the particles in the expansion, and assumes that the mass of the state is proportional to the resulting number. This works nicely for the picture of 56^+ as a $56^+ \otimes 35^-$ P-wave bound state, predicting that $(10,4)^+$ has a bigger mass than $(8,2)^+$ along with the correct strangeness ordering. If we take 70^- as a $56^+ \otimes 35^-$ S-wave state, we find in particular the following ordering of particle states: $N(10,2)^- > N(8,4)^- > Y_0^*(1,2)^- > N(8,2)^-$, where by N, Y_0, we

[17] Previous work along this line has been done by I. P. Gyuk and S. F. Tuan, Phys. Rev. **140**, B164 (1965); J. G. Belinfante, *ibid.* **140**, B154 (1965); J. G. Koerner, Northwestern University report, 1966 (unpublished), and references cited in these papers.
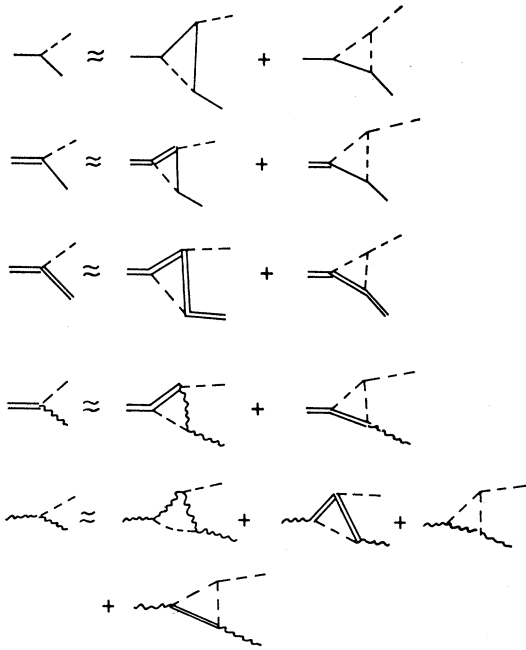
FIG. 3. Graphs in the $56^+:70^-:20^+$ vertex equations with large coefficients. Single, double, and dashed straight lines represent 56^+, 70^-, and 35^-, respectively. The curved single line represents 20^+.

mean the strangeness 0 and -1 members of the $SU(3)$ multiplets shown in the parentheses. Although there appear to be at present two potential candidates for the strangeness-zero $(8,2)^-$ slot in 70^-, neither is lighter than $Y_0^*(1405)$ and so the above qualitative prediction is incorrect. A more accurate description of the 70^- spectrum must come from a study of its coupling to both composites, $56^+ \otimes 35^-$ and $70^- \otimes 35^-$. We do this with $SU(6)$ tensor analysis,[17] concentrating on determining the effect of the meson mass splittings. If we do not take assignment mixing (discussed in Sec. 2) into account, we may accurately describe the meson spectrum for P-wave assignments with tensors transforming as 35 and 405, whereas the S-wave assignments require 35 and 189. The effect of assignment mixing is to admit small amounts of 189 mass-breaking effects into the P-wave meson spectrum. Using expressions derived by Belinfante[17] for tensors transforming as 189 and 405, we have the following relations for submultiplets of 70^-:

$$X_{405}: \quad M(8,4) = M(10,2) = M_0 + 0.85M,$$
$$M(8,2) = M_0 - 2.15M,$$
$$M(1,2) = M_0 - 5.15M. \tag{10}$$
$$X_{189}: \quad M(8,4) = M(1,2) = M_0 + 2.4N,$$
$$M(10,2) = M_0 - 3.6N,$$
$$M(8,2) = M_0 - 0.6N.$$

The main consequence of these relations is that the high mass of $(10,2)^-$ and low mass of $(1,2)^-$ can be qualitatively understood as due to a combination of the above tensors, whose origins lie in the P- and S-wave vertices. Further, this analysis points to the $N\eta$ enhancement being preferred to the more elastic entity near 1700 MeV as a candidate for 70^-. However, remembering that the mass value of a given state is properly a matter for a dynamical calculation, we feel that more work remains to be done on this important point.

4. DYNAMICS OF THE MULTIPLET 20

A. Positive Parity

There are rather strong experimental and theoretical motivations for studying the possible occurrence in nature of a positive-parity 20-dimensional multiplet of $SU(6)$. Phase-shift analyses show a strong attraction in the P_{11} state of the πN system[1,18] and production experiments indicate an enhancement in mass distribution at center-of-mass energy 1.4 BeV with the spin-parity quantum numbers of the nucleon.[19] Noting that the content of 20^+ is $(8,2)^+ \oplus (1,4)^+$, we interpret the above as evidence for the strangeness-zero number of the octet. There is no clear evidence yet of a spin-$\frac{3}{2}$ unitary singlet of positive parity, which may not be surprising if the resonance is highly inelastic with respect to pseudoscalar-meson–baryon scattering states. From our dynamical point of view, a study of the relevant $SU(6)$ crossing coefficients indicates sufficient attraction in both $70^- \otimes 35^-$ and $20^+ \otimes 35^-$ to warrant a bootstrap study of this system. The situation is not completely clear, however, since there is an ominous mutual repulsion of 20^+ and 56^+ in $70^- \otimes 35^-$ scattering whose effect can only be judged by completely solving the bootstrap equations.

In view of this $56^+:20^+$ repulsion, we first determine whether the $70^-:20^+$ system contains sufficient attraction by studying a $70^-:20^+$ bootstrap model. This model includes a mechanism for 20^+ previously advocated by Capps,[15] a $70^- \otimes 35$ composite held together by meson exchange. In addition, there are all possible meson and baryon exchanges allowed by $SU(6)$ occurring in the internal structure of the following vertices: $g_2 = (D^{(1)}{}_2)^{1/2}$ $\times g(70^-:70^-:35^-)$, $g_3 = (D^{(2)}{}_2)^{1/2} g(70^-; 20^+; 35^-)$, g_4 $= (D^{(1)}{}_2)^{1/2} g(20^+; 20^+; 35^-)$. The only mass difference occurring here is described by the parameter $x = (M[20]$ $-M[70]) D^{(2)}{}_3/D^{(2)}{}_2$. A self-consistent solution for the $70^-:20^+$ bootstrap equations exists with $g_2 = 0.69$, g_4 $= 0.82$, $g_3 = 0.46$, $x = -0.205$. These equations can be obtained from the $56:70^-:20^+$ equations [Eq. (11)] by omitting all factors referring to 56^+. We proceed immediately to a discussion of the $56^+:70^-:20^+$ system since there is no inherent interest in a $70^-:20^+$ model other than showing a 20^+ may exist at that level. In searching for a solution of the $56^+:70^-:20^+$ equations, we note that both the $56^+:70^-$ and $20^+:70^-$ models

[18] L. D. Roper, Phys. Rev. Letters 12, 340 (1964).
[19] E. W. Anderson et al., Phys. Rev. Letters 16, 855 (1966); G. Belletini et al., ibid. 15, 167 (1965); S. L. Adelman, ibid. 14, 1043 (1965).

have a solution with the **70⁻** the less tightly bound of the two. Since both **56⁺** and **20⁺** attract **70⁻** and indirectly repel each other, one expects to find a solution with the **70⁻** bound as tightly or more tightly than either the **56⁺** or the **20⁺**. This turns out to be the case as we solve the equations

$$g_0 = \frac{11}{15}g_0^3 + \frac{9}{4}\left(\frac{5}{33}\right)^{1/2}g_1^2 g_2(1-2x_1) + \frac{1}{2}\left(\frac{8}{15}\right)^{1/2}g_0^2 g_\mu + \frac{3}{8}\left(\frac{10}{3}\right)^{1/2}g_1^2 g_2(1-2x_1),$$

$$g_1 = \left[\frac{g_1^2}{4} + \frac{9}{5}\left(\frac{5}{33}\right)^{1/2}g_0 g_2 + \frac{1}{2}\left(\frac{2}{11}\right)^{1/2}g_2 g_\mu\left(1-\frac{x_1}{\gamma}\right) + \frac{3}{4}\left(\frac{8}{15}\right)^{1/2}g_0 g_\mu\left(1+\frac{x_1}{\gamma}\right) - g_3^2(1-x_1-x_2)\right]g_1,$$

$$g_2 = \frac{7}{11}g_2^3 + \frac{9}{5}\left(\frac{5}{33}\right)^{1/2}g_1^2 g_0(1+2x_1) + \left(\frac{2}{11}\right)^{1/2}g_2^2 g_\mu + \frac{1}{2}\left(\frac{2}{11}\right)^{1/2}g_1^2 g_\mu(1+2x_1)$$
$$+ \frac{5}{7}\left(\frac{7}{11}\right)^{1/2}g_3^2 g_4(1-2x_2) + \frac{3}{2}\left(\frac{2}{11}\right)^{1/2}g_3^2 g_\mu(1-2x_2),$$

$$g_3 = \left[-g_1^2(1+x_1+x_2) + \frac{5}{(77)^{1/2}}g_2 g_4 + \frac{g_3^2}{2} + \frac{3}{2}\left(\frac{2}{11}\right)^{1/2}g_2 g_\mu\left(1+\frac{x_2}{\gamma}\right) + \frac{1}{2}\left(\frac{2}{7}\right)^{1/2}g_4 g_\mu\left(1-\frac{x_2}{\gamma}\right)\right]g_3,$$

$$g_4 = \frac{3}{7}g_4^3 + \frac{5}{2}\left(\frac{7}{11}\right)^{1/2}g_3^2 g_2(1+2x_2) + \left(\frac{2}{7}\right)^{1/2}g_4^2 g_\mu + \left(\frac{7}{8}\right)^{1/2}g_3^2 g_\mu(1+2x_2),$$

$$\frac{[D^{(1)}{}_2]^2}{D^{(1)}{}_3 K_0} = \frac{11}{15}g_0^4 + \frac{1}{2}\left(\frac{8}{15}\right)^{1/2}g_0^3 g_\mu + g_1^2\left[\frac{5\gamma}{16}(1-2x_1-\eta x_1)g_1^2 + \frac{9}{4}\left(\frac{5}{33}\right)^{1/2}\gamma(1-3\eta x_1)g_0 g_2\right.$$

$$+ \frac{9}{4}\left(\frac{5}{33}\right)^{1/2}(1-2x_1)g_0 g_2 + \frac{5}{8}\left(\frac{2}{11}\right)^{1/2}\left(1-2x_1-\frac{3x_1}{\gamma}\right)g_2 g_\mu + \frac{3}{8}\left(\frac{10}{3}\right)^{1/2}\gamma(1-3\eta x_1)g_0 g_\mu$$

$$\left.+ \frac{3}{8}\left(\frac{10}{3}\right)^{1/2}(1-2x_1)g_0 g_\mu - \frac{5}{4}\gamma(1-2x_2-\eta(2x_1+x_2))g_3^2\right] \tag{11}$$

$$= \frac{7}{11}g_2^4 + \left(\frac{2}{11}\right)^{1/2}g_2^3 g_\mu + g_1^2\left[\frac{\gamma}{4}(1+\eta x_1+2x_1)g_1^2 + \frac{9}{5}\left(\frac{5}{33}\right)^{1/2}\gamma(1+3\eta x_1)g_0 g_2\right.$$

$$+ \frac{9}{5}\left(\frac{5}{33}\right)^{1/2}(1+2x_1)g_0 g_2 + \frac{3}{4}\left(\frac{8}{15}\right)^{1/2}\left(1+2x_1+\frac{3x_1}{\gamma}\right)g_0 g_\mu + \frac{1}{2}\left(\frac{2}{11}\right)^{1/2}(1+3\eta x_1)g_2 g_\mu$$

$$\left.+ \frac{1}{2}\left(\frac{2}{11}\right)^{1/2}g_2 g_\mu(1+2x_1)\right] + g_3^2\left[\frac{\gamma}{2}(1-\eta x_2-2x_2)g_3^2 + \frac{5}{7}\left(\frac{7}{11}\right)^{1/2}\gamma(1-3\eta x_2)g_2 g_4\right.$$

$$+ \frac{5}{7}\left(\frac{7}{11}\right)^{1/2}g_2 g_4(1-2x_2) - g_1^2((1+\eta(2x_1+x_2)-2x_2) + (1-\eta(2x_2+x_1)+2x_1))$$

$$\left.+ \frac{1}{2}\left(\frac{2}{7}\right)^{1/2}g_4 g_\mu\left(1-2x_2-\frac{3x_2}{\gamma}\right) + \frac{3}{2}\left(\frac{2}{11}\right)^{1/2}\gamma(1-3\eta x_2)g_2 g_\mu + \frac{3}{2}\left(\frac{2}{11}\right)^{1/2}(1-2x_2)g_2 g_\mu\right]$$

$$= \frac{3}{7}g_4^4 + g_3^2\left[\frac{7}{4}\gamma(1+2x_2+\eta x_2)g_3^2 + \frac{5}{2}\left(\frac{7}{11}\right)^{1/2}\gamma(1+3\eta x_2)g_2 g_4\right.$$

$$+ \frac{5}{2}\left(\frac{7}{11}\right)^{1/2}(1+2x_2)g_2 g_4 - \frac{7}{2}\gamma(1+2x_2+\eta(2x_2+x_1))g_1^2 + \frac{21}{4}\left(\frac{2}{11}\right)^{1/2}\left(1+2x_2+\frac{3x_2}{\gamma}\right)g_2 g_\mu$$

$$\left.+ \left(\frac{7}{8}\right)^{1/2}g_4 g_\mu \gamma(1+3\eta x_2) + \left(\frac{7}{8}\right)^{1/2}g_4 g_\mu(1+2x_2)\right] + \left(\frac{2}{7}\right)^{1/2}g_4^3 g_\mu,$$

where g_0, g_1, g_2, γ, η, g_μ are as in Sec. 3, g_3, g_4 are as defined previously in this section, $x_1 = (M[70] - M[56]) \times D^{(2)}{}_3/D^{(2)}{}_2$ and $x_2 = (M[20] - M[70])D^{(2)}{}_3/D^{(2)}{}_2$. The solution referred to above is $g_0 = 0.95$, $g_1 = 0.16$, $g_2 = 0.87$, $g_3 = 0.39$, $g_4 = 0.685$, $x_1 = -0.05$, $x_2 = -0.065$. No other solution was found. The largest terms for each vertex are shown in Fig. 3. Before examining these numerical results, we consider to what extent quantitative significance should be attached to them. The main point is that in $SU(6)$, the vertex $56^+:20^+:35^-$ is zero whereas a phenomenological coupling constant obtained from the $N^*(1400) \rightarrow N\pi$ width is fairly substantial. In view of our crude kinematics and the inadequacy of $SU(6)$ to properly describe the $56^+:20^+:35^-$ vertex, we examine the results for their qualitative features only. The most important aspect of the solution is the near degeneracy of the 56^+, 70^-, 20^+ masses, the values of x_1, x_2 corresponding to $56^+:70^-$ and $70^-:20^+$ mass differences of 53 and 65 MeV as compared to an average meson mass of 750 MeV. This means that there do exist important attractions for the 20^+ which, according to this model, are probably strong enough to produce resonances even with actual masses and coupling constants used. As before, the internal structure of the 56^+ system is a consequence mainly of self-exchange and meson-exchange processes in $56^+ \otimes 35^-$ composites. The 70^- behaves in this model in an analogous manner. However, the 20^+ is a more complicated entity, relying heavily upon both itself and 70^- in its internal structure (see Fig. 3). The array of forces seen in this $56^+:70^-:20^+$ model leads to a partial understanding of the strong inelasticity seen in meson-baryon scattering experiments in the resonance region. Inclusion of the spin-$\frac{3}{2}$ decuplet of isobars and the vector mesons into 56^+ and 35^-, respectively, along with the spin-$\frac{1}{2}$ baryons and pseudoscalar mesons implies the dynamical equivalence of all these particles and naturally explains the ease with which the former pair are produced experimentally. Study of the forces generating the 70^- multiplet not only explains the generation of most of the observed negative-parity states but also describes the inelasticity of these states relative to the original scattering states. Also, interpretation of the 20^+ as, to some extent, a baryon–two-meson composite and the importance of $70^-:20^+$ forces gives us a look at a whole range of dynamics lying outside the simple pseudoscalar-meson–baryon two-particle system.

Analysis of the "potential matrix" (described in Sec. 3) shows that the solution is self-consistent in the 56^+, 70^-, 20^+ direct channels, having eigenvalues there of $\lambda(56^+) = 1.0, 0.21$; $\lambda(70^-) = 1.0, 0.55, -0.05$; $\lambda(20^+) = 1.0, 0.21$. Anticipating the discussion of 20^- given in the next section, we also examine the potential matrix in the 20^- direct channel as reached by $70^- \otimes 35^-$ and $20^+ \otimes 35^-$ scattering. The potential matrix is now a function of the 20^- mass, so we can determine what mass value will give an eigenvalue of 1 or assume the mass to be small and determine the resulting eigen-

values. In either case, we find a large cancellation of attractive and repulsive forces such that there is no evidence for generating 20^- with the solution found in the 56^+, 70^-, 20^+ model.

B. Negative Parity

As with the 20^+, there are both experimental and theoretical reasons for considering the possible existence of a negative-parity 20. On the basis of dynamical arguments[4] and decay branching ratios, there is little doubt that the spin-$\frac{3}{2}$ $Y_0^*(1520)$ is a unitary singlet, and as mentioned previously, there appear to be two isospin-$\frac{1}{2}$ S-wave resonances in the πN system. Thus, the available states in 20^-, i.e., $(8,2)^- \oplus (1,4)^-$, have experimentally observed candidates. A study of the relevant $SU(6)$ crossing matrix elements shows that there are several attractive forces for the 20^- and no mutual $56^+:20^-$ repulsions. However, there do exist some mutually repulsive $70^-:20^-$ forces, a circumstance which makes it necessary to study first the $70^-:20^-$ system to ascertain whether the 20^- is bound (addition of 56^+ to the model will only tend to bind 70^- more tightly without affecting 20^-). This model was studied and no solutions were found, implying that the 70^- repulsions are too great to overcome. The only other possibility for generating a 20^- lies in a $56^+:70^-:20^+:20^-$ model in which the parity doublet contains strong, attractive self-exchange forces. We emphasize that even if a solution to such a model is found, it would lie far from reality in the sense that experiment implies the states we wish to put into 20^- are strongly coupled to the pseudoscalar-meson–baryon system. However, it could point to a connection between the $Y_0^*(1520)$ unitary singlet and a higher mass octet of S-wave resonances. Therefore, we have undertaken a study of the $56^+:70^-:20^+:20^-$ system and have found a solution having the following features:

(i) 56^+ and 70^- are nearly degenerate, lying roughly 300 MeV above an approximately degenerate $20^+:20^-$ parity doublet;

(ii) The $20^-:70^-:35^-$ coupling is almost zero, as expected from the above discussion.

The next step is to see how a more realistic model might affect the solution. For instance, consider how the unphysical mass difference (i) would change if the 20 states were allowed to couple to 56^+. First, the binding of the 56^+ would be strengthened by these couplings. A larger effect might come from the decreasing importance of graphs involving only $20:20:35^-$ and trimeson vertices. The trimeson vertex, an input not determined by our calculation, is the source of "regenerative feedback" effects, brought on by the importance of the meson-exchange graphs which to a large extent produce the tight binding of the $20^+:20^-$. Reduction in the relative importance of these graphs in a more realistic model might vitiate the feedback effect,

TABLE I. Born phase shifts in various partial waves of $S=1$; $T=0,1$ channels. W is the center-of-mass energy in the KN system. The states of definite angular momentum and parity are denoted by L_J, where L is the orbital angular momentum.

$S=1$ $T=0$

W (MeV)	$P_{3/2}$	$P_{1/2}$	$D_{5/2}$	$D_{3/2}$	$F_{7/2}$	$F_{5/2}$
1600	−13.0	54.6	−0.7	3.6	−0.2	0.5
1815	−33.9	big	−4.3	14.2	−2.8	4.3

$S=1$ $T=1$

W (MeV)	$P_{3/2}$	$P_{1/2}$	$D_{5/2}$	$D_{3/2}$	$F_{7/2}$	$F_{5/2}$
1600	3.6	−19.7	0.3	−2.0	0.1	−0.2
1815	4.9	−45.5	−0.6	−9.9	0.2	−1.7

thus reducing the binding of the parity doublet. Also, if we decrease the size of the input trimeson coupling[11] to correct for a possible overestimation, the binding of the parity doublet decreases relative to the $56^+:70^-$.

5. KN SCATTERING EFFECT

Structure has recently been seen in K-D scattering[20] with baryon number one, strangeness one, and isospin zero.[21] In this section we make a prediction based on long-range forces as to the spin and parity of this effect and the likelihood of observing related structure in channels of different strangeness.

Working along the lines of Ref. 4, we compute the Born phase shift for $T=0, 1$ KN scattering in states of definite angular momentum and parity as generated by the exchange of the following particles: $Y_1^*(1385)$, $Y_1^*(1660)$, Λ, Σ, $Y_0^*(1647)$, $\rho(750)$, $\phi(1020)$ (vector and tensor coupling). Noting that such an analysis cannot be trusted for S waves because of the lack of a centrifugal barrier, we plot in Table I P-, D-, and F-wave Born phase shifts. There is a large attraction in the $T=0$ $P_{1/2}$ partial wave and no similarly large value elsewhere. The main contributors to this force are the $Y_1^*(1385)$ exchange and the tensor coupling of vector-meson exchange. We therefore conclude that the $T=0$ KN system has the potential of exhibiting structure due to either a resonance in the $P_{1/2}$ channel or a sudden variation in the wave due to the opening of an inelastic channel, say K^*N, which opens just 35 MeV below the reported structure. At present, the phase-shift analysis reaches only 1600 MeV and predicts a large P wave of unknown parity since no polarization information has been obtained. It appears unlikely that a deep understanding of the $T=0$ effect will come until a phase-shift analysis is carried out at higher energies.

The $SU(3)$ classification of the $T=0$ KN system is $\overline{10}$. A natural question to pose is how large the forces are in the other $P_{1/2}$ $\overline{10}$ states and, in particular, whether

the $P_{1/2}, S=0$ effect at 1.4-BeV energy could be related.[22] Using the methods of Ref. 4, we investigated this point and found all forces at a given energy to typically be less than that occurring in the $T=0$ KN channel, the ordering being $S=0$, $T=\frac{1}{2}$; $S=-2$, $T=\frac{3}{2}$; $S=-1$, $T=1$ in decreasing strength. This analysis predicts that it is not likely that one should expect to see structure in $P_{1/2}$ $\overline{10}$ states other than the KN channel at center-of-mass energies below 1.7 BeV, which rules out the 1.4-BeV entity. Also, the forces show that the equal-spacing rule will not occur here. On the other hand, we wish to point out that there is evidence for a strangeness 0, $P_{1/2}$ resonance in the $\pi N \to \Lambda K$ reaction, which peaks at roughly 1.7 BeV with a total cross section of over 1 mb. As shown by various phenomenological analyses,[23] the $P_{1/2}$ assignment is consistent with polarization and angular-distribution measurements. The $P_{1/2}$ effects just discussed certainly warrant further study, particularly since they represent fairly strong evidence for the appearance of an $SU(3)$ family of $\overline{10}$ resonances. In view of the large mass of these states and the present uncertainty of their existence as resonances, we make no attempt to classify them according to $SU(6)$ at this time.[24]

6. CONCLUSION

In the first part of this section we list and discuss the most important of our results, and then proceed in the second part to comment on excited states of the baryon spectrum.

(1) The $SU(6)$ multiplets 56^+ and 70^- have been put on a dynamically firm footing on the basis of a self-consistent bootstrap model. In this model, the negative parity 70^- is seen to couple equally strongly to S-wave $56^+ \otimes 35^-$ and P-wave $70^- \otimes 35^-$ composites. The next step in understanding the physics of these multiplets is the abandonment of a strict $SU(6)$ description with the introduction of mass nondegeneracy in a given multiplet and coupling-constant deviations from $SU(6)$ values. A brief study carried out in Sec. 3 indicates the qualitative success of such a program. A further consequence of this model is that dynamics of the baryon spectrum relies upon both baryon- and meson-exchange processes and any calculation which omits either is likely to prove inadequate.[10]

(2) A positive parity 20 can be dynamically generated in a 56^+, 70^-, 20^+ bootstrap model. The correspondence of this model with reality suffers from the lack of a $56^+:20^+:35^-$ coupling in $SU(6)$, but there is strong evidence for suspecting the existence of 20^+ in nature.

[20] R. L. Cool *et al.*, Bull. Am. Phys. Soc. **11**, 326 (1966); Phys. Rev. Letters **17**, 102 (1966).

[21] There is also possible structure in the $T=1$ channel but this can only be ascertained after much more careful treatment of the data. Note that in Table I there are no strongly attractive forces for $T=1$, implying that any structure is probably related to isobar production.

[22] C. Lovelace, CERN report, 1965 (unpublished).

[23] G. T. Hoff, Phys. Rev. **139**, B671 (1965); H. Thom, *ibid.* **151**, 1322 (1966).

[24] However, we note that the multiplet **700** contains an antidecuplet of $P_{1/2}$ states and that use of the wave-function approach for determining mass splittings (described in this paper) applied to $700 \subset 56 \otimes 35$ indicates the $P_{1/2}$ $\overline{10}$ particles would have lower mass than any other states in **700**.

In particular, we assign the P_{11} $N^*(1480)$ effect to this multiplet. We wish to point out that the πN P_{11} amplitude contains both a probable resonating part as well as a strong, highly absorptive background, and further phenomenological analysis is necessary to produce a full comprehension of this complex situation. The success of the 56^+, 70^-, 20^+ model points to important forces in multimeson-baryon systems, thus helping us to understand the large amount of inelasticity present in the resonance region.

The main purpose of our study of 20^- was to investigate the possibility of relating the $Y_0^*(1520)$ unitary singlet to an octet of S-wave resonances containing $N^*(1700)$. Subsequent discovery of a solution to the $56^+:70^-:20^+:20^-$ model rasies the intriguing possibility of explaining all baryon states of spin$\leq\frac{3}{2}$ and mass<1.7 BeV by means of four multiplets of particles. The next, essential, step is to explain how the 20^- states could become strongly coupled to the pseudoscalar-meson–baryon system.

(3) On the basis of a study of long-range forces in pseudoscalar-meson–baryon scattering with real masses and $SU(3)$ coupling constants, we predict a $P_{1/2}$ effect in the isospin-zero KN system. Examination of $\bar{10}$ states in channels of differing strangeness shows the decuplet equal spacing behavior does *not* hold here, and the $S=0$ forces are not strong enough to generate the Roper effect. However, there may be a $P_{1/2}$ $\bar{10}$ resonance with zero strangeness which appears as a peak in the $\pi N \to \Lambda K$ cross section at roughly 1700 MeV.

We conclude with remarks on excited states in the baryon spectrum. Probably the chief motivation for this paper is an attempt to explain as many as possible of the baryon states with spin $\leq\frac{3}{2}$ by means of a few fundamental entities, and we use group theory to accomplish this. At present there appears to be no group-theoretic way for describing the high-spin states. Seemingly $SU(6)\otimes O(3)$, in which one vectorially adds angular momenta $J=1, 2, 3, \cdots$ to an $SU(6)$ ground-state angular momentum, gives far too many states to fit the observed pattern. However, in analogy with previous work done using $SU(2)^3$ and $SU(3)^4$, we may be able to predict which "excited states" of our ground state are likely to appear. It can be shown for pseudoscalar-meson–baryon systems[4] that a potential arising from single-particle exchange processes which is attractive for some orbital angular momentum L will also produce attraction for states of $L+2, L+4, \cdots$ with decreasing strength at a given energy due to centrifugal barrier effects. That is, the $\Delta J=2$ recurrence picture of the baryon states in a natural consequence of the exchange forces. Conjecturing this to be true for the general spin case, the P-wave $56^+:56^+:35^-$ vertex becomes an F-wave interaction. The spin $(\frac{5}{2})^+$ octet thereupon predicted has been experimentally verified and at least two members of the spin $(\frac{7}{2})^+$ decuplet have been detected. The excitation energy here is

roughly 700 MeV. The excited 70^- has at this time at least two experimentally observed candidates, the $(\frac{7}{2})^-$ $N^*(2190)$ and $(\frac{7}{2})^-$ $Y_1^*(2260)$, which we interpret as excited states of the spin-$\frac{3}{2}$ particles $N^*(1520)$ and $Y_1^*(1660)$. The $S=0$, D_{15} resonance at 1700 MeV can be interpreted as an excited state of S_{11} $N^*(1500)$ only if there is a mechanism for explaining the abnormally low mass of D_{15} and the high mass of S_{11}. Recently Auvil and Brehm have analyzed the D_{15} using a Cook-Lee type approach with an S-wave $N^*(1238)$ $-\rho$ final state. This non-$SU(6)$ mechanism could conceivably lower the D_{15} mass by several hundred MeV. It is possible that $SU(6)$ symmetry-breaking effects can in part explain the high mass of the S_{11} particularly if the coupling-constant deviations which couple this and sister states so strongly to η-baryon composites are taken into account.

APPENDIX A: EVALUATION OF CERTAIN CROSSING COEFFICIENTS

We exhibit here techniques employed in evaluating inelastic crossing coefficients. Since we assign the mesons to 35, the regular representation of $SU(6)$, and consider only the antisymmetric coupling of 70^- to $70^-\otimes 35^-$, the Clebsch-Gordan coefficients, $C_{ab}{}^\alpha$, describing the vertex $R\subset R\otimes 35^-$, where $R=20, 56, 70$, are proportional to the generators $G_{ab}{}^\alpha$ of $SU(6)$. We use Greek indices for states belonging to 35 and Latin indices for states of $56, 70, 20$. The proportionality is fixed by adopting a particular normalization for the Clebsch-Gordan coefficients. In particular, if

$$C_{ab}{}^\alpha C_{ab}{}^\alpha = d_\alpha, \tag{A1}$$

where d_α is the dimensionality of the multiplet to which state α belongs, we have the symmetry relation,

$$C_{ab}{}^\alpha = (d_\alpha/d_a)^{1/2} C_{ab}{}^\alpha, \tag{A2}$$

where the phase has been chosen positive. The second-order Casimir operator and the "square" of the group generators are related:

$$\text{Tr}\mathbf{G}^2 = G^2(a)d_a. \tag{A3}$$

From (A1) and (A3),

$$G_{ab}{}^\alpha = ((d_a/d_\alpha)G^2(a))^{1/2} C_{ab}{}^\alpha. \tag{A4}$$

FIG. 4. (a) Diagrammatic representation of projection operator. (b) Crossing coefficient describing projection of crossed-channel state r into direct-channel state x. The states b, x belong to the same irreducible representation as do the states r, a. (c) Crossing coefficient upon reshuffling of indices, corresponding to the analytical expression (A6).
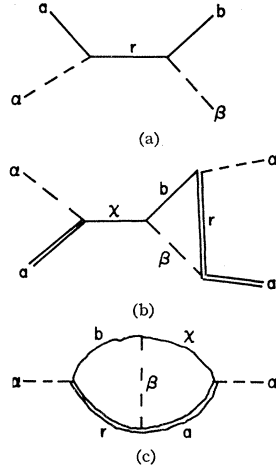
Hereafter, $C_{ab}{}^{\alpha}$ stands for an arbitrary Clebsch-Gordan coefficient, proportional to a generator only when specified.

With our normalization, the projection operator, $P_{b\beta,a\alpha}$, shown in Fig. 4(a) has the form

$$P_{b\beta,a\alpha}=C_{b\beta}{}^{r}C_{a\alpha}{}^{r}.$$

The projection of a state r belonging to multiplet R in a crossed channel to state x belonging to multiplet X in the direct channel is described by the crossing matrix element A, which is evaluated as follows:

$$C_{b\delta}{}^{r}C_{\beta d}{}^{r}=AC_{d\delta}{}^{x}C_{b\beta}{}^{x}+\cdots ,$$
$$C_{a\alpha}{}^{x}C_{b\beta}{}^{x}C_{b\delta}{}^{r}C_{\beta d}{}^{r}=AC_{a\alpha}{}^{y}C_{d\delta}{}^{y},\qquad (A5)$$
$$A=C_{a\alpha}{}^{x}C_{b\beta}{}^{x}C_{ba}{}^{r}C_{\beta a}{}^{r}/d_{\alpha}.$$

Consider evaluation of the class of crossing coefficients shown in Fig. 4(b). By a shuffling of indices using (A2), we may express the crossing coefficient in the form seen in Fig. 4(c), which corresponds to the analytical expression

$$A=(d_b/d_{\alpha}{}^2)C_{ba}{}^{\beta}[C_{ax}{}^{\alpha}C_{br}{}^{\alpha}]C_{ra}{}^{\beta}.\qquad (A6)$$

Using relation (A4), we may express (A6) as

$$A=\left(\frac{d_b}{d_a}\right)^{1/2}[G^2(a)G^2(b)]^{-1/2}\left[\frac{G^2(\alpha)-G^2(a)-G^2(b)}{2}\right].\qquad (A7)$$

Throughout our calculations, we choose the phase of (A7) to give positive values for the coupling constants.

APPENDIX B: EVALUATION OF A DYNAMICAL FACTOR

For definiteness, consider a vertex consisting of two baryonic particles of opposite relative parity and an S-wave pseudoscalar meson. We first treat the angular-momentum decomposition of the vertex, starting with the interaction term

$$g\bar{\psi}_{-}\psi_{+}\phi+\text{H.c.},\qquad (B1)$$

where we temporarily ignore internal symmetries. A momentum-space decomposition in a Cartesian basis yields in the baryonic spin space

$$g\sum_{\mathbf{k}}\frac{v(\mathbf{k})}{(2\omega V)^{1/2}}\phi_{\mathbf{k}}+\text{H.c.},\qquad (B2)$$

where $v(\mathbf{k})$ describes the baryon structure in the static limit, $\omega(\mathbf{k})=(k^2+u^2)^{1/2}$ is the pion energy, and $V=$ volume of box quantization. Expanding $\phi_{\mathbf{k}}$ in a spherical basis, we have

$$\varphi_{\mathbf{k}}=\frac{1}{k}\left(\frac{(2\pi)^3}{V}\right)^{1/2}\left(\frac{R}{\pi}\right)^{1/2}\sum_{m,l}(-i)^l Y_l{}^m(\Omega_{\mathbf{k}})\alpha_l{}^m(k),\qquad (B3)$$

where R is the radius of sphere quantization. Then we have

$$\frac{g}{V}(2\pi)^{3/2}\sum_{\mathbf{k},l,m}\frac{v(k)}{k\omega^{1/2}}(-i)^l Y_l{}^m(\Omega_{\mathbf{k}})\alpha_l{}^m(k)$$
$$=\frac{gR^{1/2}}{4\pi^2}\int\frac{d^3k}{k\omega^{1/2}}v(k)\sum_{l,m}(-i)^l Y_l{}^m(\Omega_{\mathbf{k}})\alpha_l{}^m(k),\qquad (B4)$$

noting that $\sum_{\mathbf{k}}\rightarrow V(2\pi)^{-3}\int d^3k$. Thereupon,

$$\frac{g}{(4\pi^2)^{1/2}}\left(\frac{R}{\pi}\right)^{1/2}\int_0^{\infty}\frac{kdk}{\omega^{1/2}}v(k)\alpha_0{}^0(k).\qquad (B5)$$

We now consider a particular term in the expansion of an S-wave vertex as shown in Fig. 5(a). Considering
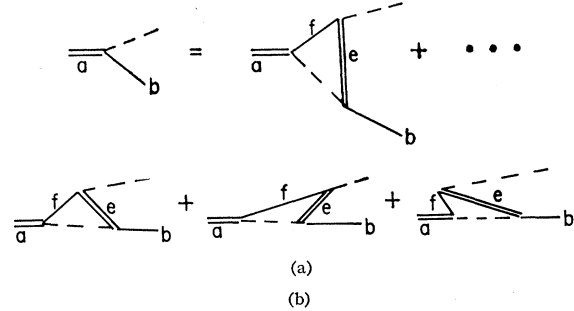
FIG. 5. (a) S-wave $70^-{:}56^+{:}35^-$ vertex along with a particular contribution. (b) Three time orderings of vertex contribution shown in (a).

only the contribution of the first time-ordered process shown in Fig. 5(b), the dynamical factor has the form

$$(4\pi^2)^{-1/2}\frac{qv(q)}{\omega^{1/2}}G_{abg}(70{:}56{:}35)$$
$$=(4\pi^2)^{-1/2}\frac{qv(q)}{\omega^{1/2}}\frac{G_{af}G_{ef}G_{eb}}{4\pi^2}\int_0^{\infty}\frac{v^2(k)k^2dk}{\omega}$$
$$\times\frac{g^3(70{:}56{:}35)}{(\omega+M_f-M_a)(\omega+M_e-M_b)}+\cdots,\qquad (B6)$$

which reduces to

$$g(70:56:35) = \frac{1}{4\pi^2} \int_\mu^\Lambda \frac{k d\omega}{(\omega + M_f - M_a)(\omega + M_e - M_b)}$$

$$\times \frac{g^3(70:56:35)}{4} + \cdots , \quad (B7)$$

where the factor of $\frac{1}{4}$ is the relevant $SU(6)$ crossing coefficient for this process. We consistently neglect contributions of baryon-exchange graphs corresponding to the latter two time orderings since such graphs are notorious for giving unrealistically large forces in a study of single-particle exchange processes.

APPENDIX C: COMPARISON OF $SU(6)$ PREDICTIONS WITH SOME EXPERIMENTAL DECAY WIDTHS

Since comparison of $56^+:56^+:35^-$ coupling constants with experiment has been treated rather extensively in the literature, we restrict ourselves to decays of the 70^- multiplet. In order to systematically relate decays into final baryonic states of spin $\frac{1}{2}$ and $\frac{3}{2}$, we use the results of free-field Lagrangians.[25] With the notation J^p (initial baryon) $\rightarrow J^p$ (final baryon)$+J^p$ (final meson), we have

$\frac{1}{2}^- \rightarrow \frac{1}{2}^+ 0^-$:

$$\frac{g^2}{4\pi} = \frac{M_R}{k} \frac{\Gamma}{E+M} . \quad (C1)$$

$\frac{3}{2}^- \rightarrow \frac{3}{2}^+ 0^-$:

$$\frac{g^2}{4\pi} = \frac{3M_r}{k} \frac{\Gamma}{[3(E+M)+(2k^2/3M^2)(E+2M)]} . \quad (C2)$$

$\frac{3}{2}^- \rightarrow \frac{1}{2}^- 0^-$:

$$\frac{g^2}{4\pi} = \frac{3M_r}{k^3} \frac{\Gamma}{E+M} , \quad (C3)$$

---

[25] J. G. Rushbrooke, Phys. Rev. **143**, 1345 (1966).

TABLE II. Comparison of experimental and $SU(6)$ coupling constants of 70^-. M_R is the mass of the decaying state given in pion masses and Γ is the partial width. The experimental values used are taken from references.

Decay	M_R (M_π)	Γ (MeV)	$\frac{g^2}{4\pi}$(expt.)	$\frac{g^2}{4\pi}(SU(6))$[a]
N_{11}^+ (1557) $\rightarrow N\pi$	11.2	110	0.06	0.06
N_{11}^+ (1700) $\rightarrow N\pi$	12.2	210	0.09	0.06
N_{31}^+ (1690) $\rightarrow N\pi$	12.1	130	0.10	0.09
Y_0^+ (1405) $\rightarrow \pi$	10.1	35	0.045	0.045
Y_1^+ (1660) $\rightarrow Y_1^+$(1385)π	11.9	8	0.01	0.03
Ξ^+ (1820) $\rightarrow \Xi^+$ (1530)π	13.0	4	0.003	0.03
N_{13}^+ (1525) $\rightarrow N^+$ (1238)π	10.9	25	0.03	0.12

[a] Normalized to correct Y_0^+ (1405) value.

where $M=$ mass of final baryon, $M_r=$ mass of resonance, $\Gamma=$ partial decay width, $E=$ energy of final baryon in resonance rest system, and $k=$ momentum of decay particles in resonance rest system.

The experimental values and corresponding coupling constants are shown in Table II. Since there is evidence for two S-wave resonances of isospin $\frac{1}{2}$ in the πN system, we have assumed each to belong to 70^- for comparison. The resonance parameters for these states are taken from Refs. 1 and 26. In general, the numbers in Table II indicate order-of-magnitude agreement between $SU(6)$ and experiment. The two S_{11} N^* resonances each give a reasonable fit to the experimental $N\pi$ partial width, so there is no reason to reject either on this basis. Decay of this state into the $N\eta$ channel is forbidden by $SU(6)$. No information is available on the $N^*(1700) \rightarrow N\eta$ partial width although this resonance appears to be rather elastic with respect to the $N\pi$ system. However, $N^*(1557)$ decays strongly into $N\eta$, having a phenomenological coupling constant $g^2(N^*N\eta)/4\pi = 0.16$. Therefore, examination of coupling constants favors slightly the assignment of $N^*(1700)$ to 70^- over $N^*(1557)$, although in view of the over-all deviation from $SU(6)$ predictions, this result is not convincing.

---

[26] F. Uchiyama-Campbell and R. K. Logan, Phys. Rev. **149**, 1220 (1966); A. H. Rosenfeld et al., University of California Laboratory Report No. UCRL 8030, revised, April 1966 (unpublished).